Synthesis, Crystal Structure and Properties of a New Lanthanide Pyridine-2,4,6-tricarboxylato Coordination Polymer

Jian-Li Lin, Wei Xu, Li Zhao, and Yue-Qing Zheng

Center of Applied Solid State Chemistry Research, Ningbo University, Ningbo, 315211, P. R. China

Reprint requests to Prof. Dr. Yue-Qing Zheng. Fax: Int. +574/87600747.
E-mail: yqzhengmc@163.com

A new lanthanide pyridine-2,4,6-tricarboxylato coordination polymer, $[Dy_2(H_2O)_5(ptc)_2]\cdot H_2O$ (H_3ptc = pyridine-2,4,6-tricarboxylic acid), was hydrothermally synthesized. The complex exhibits both mono-capped square antiprismatic $DyNO_8$ chromophores and 4,4'-bicapped trigonal prismatic $DyNO_7$ chromophores, which are interconnected through ptc^{3-} anions in $\mu_3\eta^6$ and $\mu_4\eta^6$ coordination modes to achieve a new 3D MOF of an unprecedented topology of $(4\cdot6^3\cdot8^2)(6^3)$ type. This Dy(III) complex exhibits a characteristic luminescence in the visible region upon excitation at 300 nm. The temperature-dependent magnetic properties of the Dy(III) complex were investigated in the temperature range of 2 – 300 K.

Key words: Lanthanide, Pyridine-2,4,6-tricarboxylic Acid, Coordination Polymer, Crystal Structure, Properties

Introduction

Owing to their unique spectroscopic and electronic characteristics associated with their $4f^n$ electronic configuration, lanthanide ions are widely employed for design and rational synthesis of lanthanide complexes with intriguing topological architectures and interesting properties which have promising applications in many fields such as optics, electronics, mechanics, membranes, protective coatings, catalysis, sensors, biology, *etc.* [1 – 5]. For the self-assembly of lanthanide complexes, various carboxylic acids have been extensively utilized, and many lanthanide carboxylate complexes have been reported over the past 30 years, in which the lanthanide ions show regular coordination characteristics and the carboxylate ligands exhibit different coordination modes Lanthanide carboxylate complexes display various interesting structural topologies and luminescent properties [6 – 9]. Studies have been focused in particular on the design and assembly of lanthanide complexes with aromatic carboxylic acids which have been found to be suitable ligands, for example, for terbium and dysprosium ions, because of the energy match between their triplet state levels and resonant energy levels of the central lanthanide ions [10 – 13]. Lanthanide complexes with aromatic carboxylic acids show higher thermal or luminescence stabilities for practical application than other lanthanide complex systems.
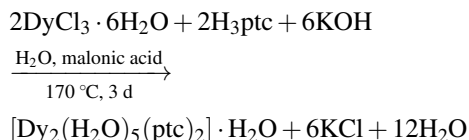
Among the aromatic carboxylic acids, the pyridine-2,4,6-tricarboxylic acid (H_3ptc) can form conjugated structures with both N and O donor atoms. It can act as a multidentate ligand as well as a bridging linker for the design of metal-organic molecular assemblies [14 – 18]. As part of our ongoing research [19, 20] pyridine-2,4,6-tricarboxylic acid (H_3ptc) was employed to construct novel coordination polymers. Herein, we report the new lanthanide pyridine-2,4,6-tricarboxylato complex $[Dy_2(H_2O)_5(ptc)_2]\cdot H_2O$.

Results and Discussion

Syntheses

In the presence of malonic acid, $DyCl_3\cdot6H_2O$ and H_3ptc react hydrothermally in an aqueous KOH solution to give $[Dy_2(H_2O)_5(ptc)_2]\cdot H_2O$. Repeated experiments indicated that malonic acid is essential for a successful synthesis of the title complex. The phase purity of the crystalline product was confirmed by comparing an experimental powder X-ray diffraction (PXRD) pattern with the corresponding one simulated on the basis of the single-crystal data (Fig. 1) as well as by an elemental analysis. The above synthetic reaction could be

expressed by the following equation:

$$2DyCl_3 \cdot 6H_2O + 2H_3ptc + 6KOH$$

$$\xrightarrow[\text{170 °C, 3 d}]{\text{H}_2\text{O, malonic acid}}$$

$$[Dy_2(H_2O)_5(ptc)_2] \cdot H_2O + 6KCl + 12H_2O$$

The title compound was found to be stable in air and insoluble in common solvents such as water, ethanol, and acetone.

Description of the crystal structure

In the asymmetric unit of the title complex there are two Dy^{3+} ions (Dy1 and Dy2), two ptc^{3-} ions, five aqua ligands (O7, O8, O9, O16 and O17) and one additional water molecule (O10). As demonstrated in Fig. 2, the N1-containing ptc^{3-} ion as a $\mu_4\eta^6$ bridging ligand is bonded to two Dy1 atoms through the pyridyl N atom and its two neighboring carboxylate O atoms in a chelating/bridging mode and to two Dy2 atoms through the 4-position carboxylate group in a $\mu_2\eta^2$-syn-syn mode. The N2-containing ptc^{3-} ion acts as a $\mu_3\eta^6$ bridging ligand to chelate one Dy1 through the 4-position carboxylate group and coordinates two Dy2 atoms through the pyridyl N atom and its two neighboring carboxylate O atoms in a chelating/bridging mode. It should be pointed out that the present $\mu_3\eta^6$ and $\mu_4\eta^6$ bridging modes of the ptc^{3-} ligands, to the best of our knowledge, are unprecedented. The coordination effects destroy the coplanarity of the ptc^{3-} anions, and the distortion of the $\mu_4\eta^6$ptc ligand is more significant than that of the $\mu_3\eta^6$ptc ligand, the dihedral angles between the carboxyl group and the pyridine ring being 16.3(4)°, 42.2(2)°, and 12.7(5)°, respectively, for the C1-, C3- and C5-bonded carboxyl groups in the $\mu_4\eta^6$ptc ligand, and 2.1(5)°, 17.1(2)°, and 2.2(4)°, respectively, for the C9-, C11- and C13-bonded carboxyl groups in the $\mu_4\eta^6$ptc ligand.

The Dy1 atoms are coordinated by three aqua ligands (O7, O8 and O9) as well as one $\mu_3\eta^6$ and two $\mu_4\eta^6$ptc ligands to generate a distorted mono-capped square antiprismatic $DyNO_8$ chromophore with $d(Dy-N) = 2.476(4)$ Å and $d(Dy-O) = 2.381 - 2.608$ Å. The Dy2 atoms are complexed by two aqua ligands (O16 and O17) as well as one $\mu_4\eta^6$ and two $\mu_3\eta^6$ ptc ligands to complete a distorted 4,4'-bicapped trigonal prismatic $DyNO_7$ coordination sphere with $d(Dy-N) = 2.470(4)$ Å and $d(Dy-O) = 2.312 - 2.432$ Å (Table 1).

For convenience of understanding the crystal structure of the title compound, the O4-Dy2[#3] bonding in-
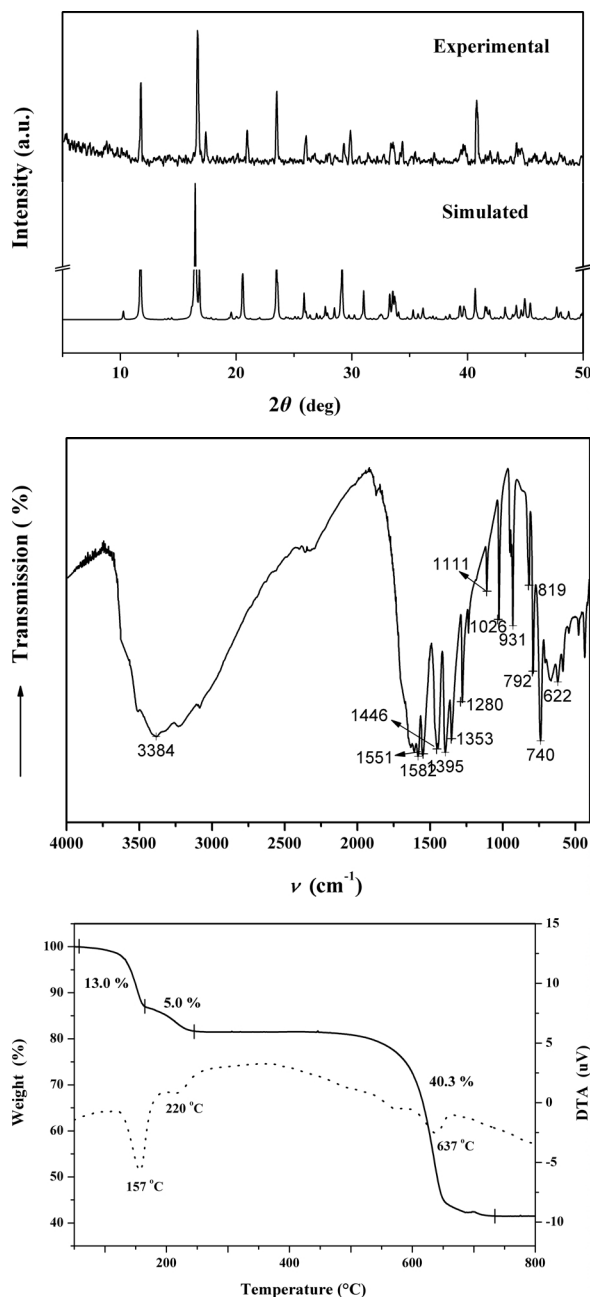

Fig. 1. Experimental and simulated PXRD patterns (top), infrared spectrum (middle), and TG curve (bottom) for the title compound.

teraction ([#3] $-x + 1$, $-y + 1$, $-z + 1$) and its symmetry equivalents are tentatively not taken into consideration. The lanthanide atoms are then interconnected by both $\mu_3\eta^6$ and $\mu_4\eta^6$ptc ligands to afford 2D corrugated layers (Fig. 3a). The layers extend in-

Table 1. Selected bond lengths (Å), angles (deg) and hydrogen bonding contacts for **1** with estimated standard deviations in parentheses[a].

Distances					O6–Dy1–O12	68.2(1)	O10#4–Dy2–O15	92.3(1)
Dy1–O1#1	2.510(3)	Dy2–O3#2	2.393(3)		O6–Dy1–O13	120.3(1)	O10#4–Dy2–O16	68.1(1)
Dy1–O2	2.423(3)	Dy2–O4#3	2.364(3)		O6–Dy1–N1	65.3(1)	O10#4–Dy2–O17	93.6(1)
Dy1–O6	2.382(3)	Dy2–O10#4	2.343(3)		O7–Dy1–O8	142.7(1)	O10#4–Dy2–N2	73.1(1)
Dy1–O7	2.398(3)	Dy2–O11	2.432(3)		O7–Dy1–O9	73.5(1)	O11–Dy2–O15	130.3(1)
Dy1–O8	2.381(3)	Dy2–O15	2.367(3)		O7–Dy1–O12	134.8(1)	O11–Dy2–O16	133.9(1)
Dy1–O9	2.398(3)	Dy2–O16	2.415(3)		O7–Dy1–O13	138.9(1)	O11–Dy2–O17	71.8(1)
Dy1–O12	2.608(4)	Dy2–O17	2.312(4)		O7–Dy1–N1	71.7(1)	O11–Dy2–N2	64.3(1)
Dy1–O13	2.442(3)	Dy2–N2	2.470(4)		O8–Dy1–O9	139.6(1)	O15–Dy2–O16	79.8(1)
Dy1–N1	2.476(4)				O8–Dy1–O12	70.1(1)	O15–Dy2–O17	158.0(1)
Angles					O8–Dy1–O13	76.9(1)	O15–Dy2–N2	66.0(1)
O1#1–Dy1–O2	71.0(1)	O9–Dy1–N1	135.2(1)		O8–Dy1–N1	71.2(1)	O16–Dy2–O17	82.7(1)
O1#1–Dy1–O6	146.7(1)	O12–Dy1–O13	52.2(1)		O9–Dy1–O12	69.7(1)	O16–Dy2–N2	126.3(1)
O1#1–Dy1–O7	72.2(1)	O12–Dy1–N1	120.3(1)		O9–Dy1–O13	75.8(1)	O17–Dy2–N2	135.9(1)
O1#1–Dy1–O8	127.4(1)	O13–Dy1–N1	147.2(1)					
O1#1–Dy1–O9	69.7(1)	O3#2–Dy2–O4#3	73.1(1)		Hydrogen bonding contacts			
O1#1–Dy1–O12	116.4(1)	O3#2–Dy2–O10#4	138.1(1)		D–H···A	d(D–H) d(H···A) d(D–H···A)	∠(D–H···A)	
O1#1–Dy1–O13	71.8(1)	O3#2–Dy2–O11	133.9(1)		O7–H7A···O14#5	0.83 1.83 2.651(4)	172	
O1#1–Dy1–N1	123.1(1)	O3#2–Dy2–O15	80.8(1)		O7–H7B···O2#1	0.89 1.81 2.672(4)	166	
O2–Dy1–O6	129.2(1)	O3#2–Dy2–O16	70.0(1)		O8–H8A···O12#3	0.73 2.06 2.787(5)	175	
O2–Dy1–O7	86.1(1)	O3#2–Dy2–O17	80.7(1)		O8–H8B···O9#6	0.76 2.26 2.837(4)	135	
O2–Dy1–O8	74.5(1)	O3#2–Dy2–N2	136.5(1)		O9–H9A···O5#5	0.86 2.58 3.036(5)	114	
O2–Dy1–O9	139.6(1)	O4#3–Dy2–O10#4	148.3(1)		O9–H9B···O5#5	0.86 2.61 3.036(4)	112	
O2–Dy1–O12	139.1(1)	O4#3–Dy2–O11	80.3(1)		O9–H9B···O6#5	0.86 1.91 3.039(4)	115	
O2–Dy1–O13	100.3(1)	O4#3–Dy2–O15	87.6(1)		O16–H16A···O4#5	0.85 2.29 3.083(4)	156	
O2–Dy1–N1	64.1(1)	O4#3–Dy2–O16	142.4(1)		O16–H16B···O15#7	0.83 1.98 2.806(4)	171	
O6–Dy1–O7	82.3(1)	O4#3–Dy2–O17	98.3(1)		O17–H17A···O18#4	0.88 1.82 2.690(5)	173	
O6–Dy1–O8	85.8(1)	O4#3–Dy2–N2	78.0(1)		O17–H17B···O5#8	0.85 1.97 2.793(5)	165	
O6–Dy1–O9	83.0(1)	O10#4–Dy2–O11	75.7(1)		O18–H18A···O14#9	0.81 2.13 2.944(5)	176	
					O18–H18B···O13	0.84 1.93 2.753(5)	167	

[a] Symmetry transformations used to generate equivalent atoms: #1 $-x+1/2, y-1/2, -z+1/2$; #2 $x, y, z+1$; #3 $-x+1, -y+1, -z+1$; #4 $-x+1/2, y-1/2, -z+3/2$; #5 $-x+1, -y, -z+1$; #6 $x, y+1, z$; #7 $-x+1, -y, -z+2$; #8 $x-1/2, -y+1/2, z+1/2$; #9 $x-1/2, -y+1/2, z-1/2$.
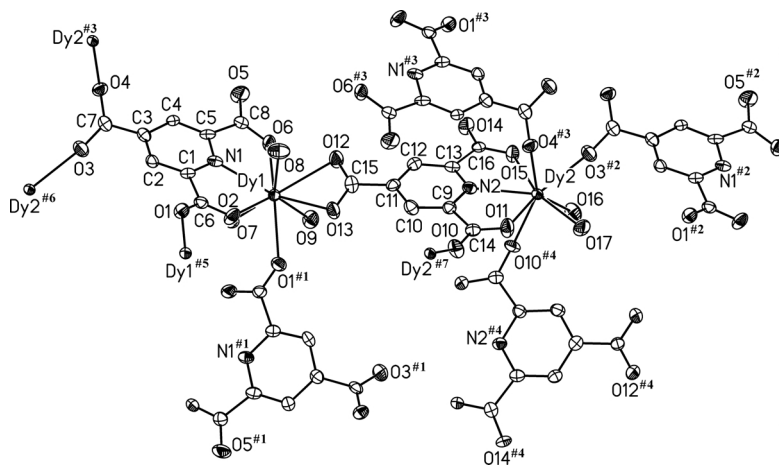

Fig. 2. ORTEP view of coordination environments of the Dy atoms and the bridging modes of the ptc[3−] ligands in the title compound together with the atom numbering scheme and the displacement ellipsoids drawn at 45 % probability level. Symmetry transformations used to generate equivalent atoms: #1 $-x+1/2, y-1/2, -z+1/2$; #2 $x, y, z+1$; #3 $-x+1, -y+1, -z+1$; #4 $-x+1/2, y-1/2, -z+3/2$; #5 $-x+1/2, y+1/2, -z+1/2$; #6 $x, y, z-1$; #7 $-x+1/2, y+1/2, -z+3/2$.

finitely parallel to the (100) plane, and the adjacent layers are centrosymmetrically related to one another. In an approximation, the 2D layer can be simplified to a (4,4) net. Through the O4-Dy2#3 bonding inter- action (#3 $-x+1, -y+1, -z+1$) and its symmetry-equivalents, the 2D layers are interlinked to generate a 3D MOF (Fig. 3b). The structure of the title compound is actually rather intricate. The two crystallographi-
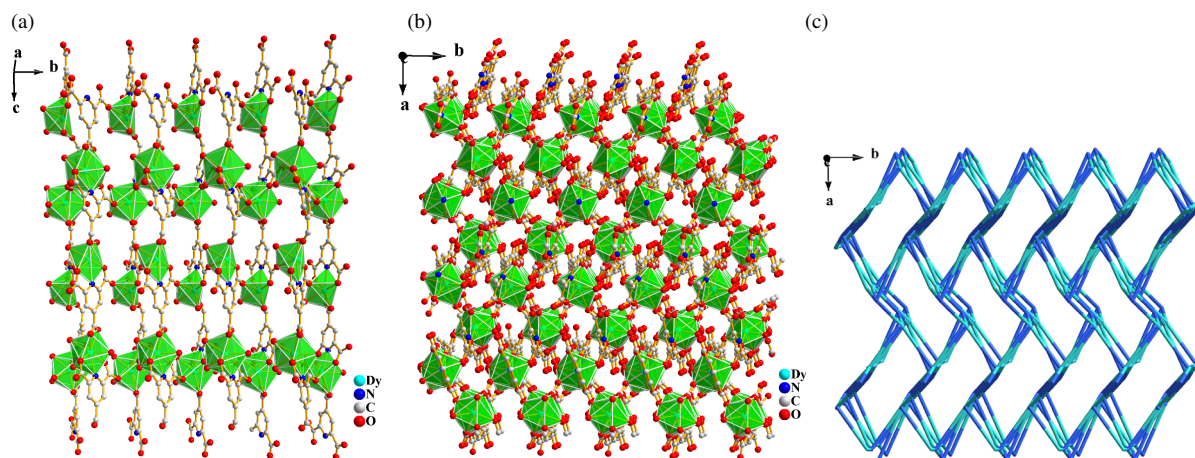
Fig. 3 (color online). (a) A layer generated from Dy^{3+} ions bridged by ptc^{3-} ligands; (b) 3D MOF structure; (c) a topological representation $(4 \cdot 6^3 \cdot 8^2)(6^3)$ of the title complex.

cally distinct ptc ligands bridge three and four metal atoms, and the Dy1 and Dy2 atoms are coordinated to three and four ptc ligands, respectively. Therefore, Dy1, Dy2 and the $\mu_3\eta^6$ptc and $\mu_4\eta^6$ptc ligands could be treated as three-, four-, four- and three-connected nodes, and the present 3D MOF can be simplified to a novel herringbone-like $(4 \cdot 6^3 \cdot 8^2)(6^3)$ topology (Fig. 3c).

The aquo ligands donate hydrogen atoms to the carboxylate O atoms to form abundant hydrogen bonds (Table 1), which make substantial contributions to the stability of the crystal structure. The solvate water molecules are located in cavities and are hydrogen-bonded to the framework.

Infrared spectra

As illustrated in Fig. 1, the infrared spectrum of the title complex shows characteristic broad bands centered at 3384 cm^{-1}, due to the absorption from OH stretching vibrations of the water molecules [21]. The sharp peaks at 1582, 1446 and 1395 cm^{-1} can be assigned to the asymmetric (ν_{as}) and symmetric (ν_{sy})-COO stretching vibrations, respectively, and the differences $\Delta\nu_{as} - \Delta\nu_{sy}$ of 187 and 51, respectively, suggest that the -COO groups are coordinated to metal ions in mono- and bidentate modes. The absorptions in the range 740–1026 cm^{-1} can be attributed to the skeleton vibrations of the organic ligand.

Thermal analysis

The DTA curve (Fig. 1) for the title compound shows three endothermic peaks at 157, 220 and 637 °C.

The TG curve indicates that the first weight loss of 13.0 % in the range 75–170 °C corresponds well to the removal of one solvate water molecule and five aquo ligands (calcd. 12.7 %). The dehydrated intermediate may be "$Dy_2(ptc)_2$", which experiences slight weight loss of 5.0 % over 170–250 °C close to the value of 5.2 % for liberation of one carboxyl group (COO). The sample then undergoes rapid decomposition with an additional weight loss of 40.3 %. The weight of the residue at 710 °C remains at 41.7 %, which is slightly less than the value of 43.9 % for Dy_2O_3, indicating a substantial loss of the Dy element during the last almost explosive stage.

Fluorescent properties

The emission spectrum of the title compound in the solid state was determined upon excitation at 300 nm at ambient temperature (Fig. 4). The complex is blue luminescent and displays the characteristic Dy^{3+} emission. The two peaks at 482 and 573 nm are due to the magnetic dipole transition $^4F_{9/2} \rightarrow {}^6H_{15/2}$ (blue emission) and the electric dipole transition $^4F_{9/2} \rightarrow {}^6H_{13/2}$ (yellow emission) of the Dy^{3+} ion. The emission intensity generally varies with the change of the coordination environment of the metal ions, and the ratio of yellow emission and blue emission (Y/B) is a measure of the site symmetry at which the Dy^{3+} ion is situated [22]. For the title compound the Y/B value is 0.80, indicating a slight lowering of the local Dy^{3+} site symmetry from an inversion center in good agreement with the result of X-ray single-crystal diffrac-
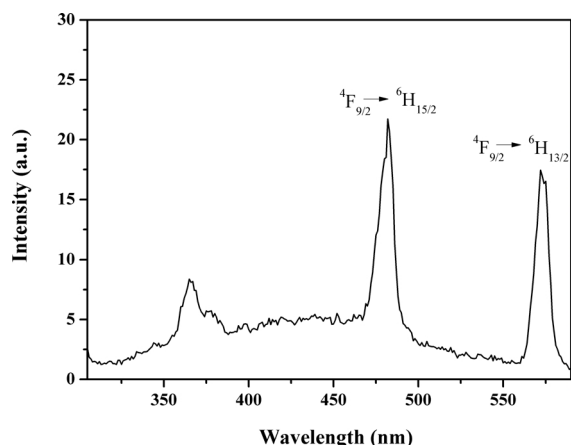
Fig. 4. Emission spectrum of the title compound in the solid state at room temperature (λ_{ex} = 300 nm).

tion. The strongest emission band is located at 482 nm ($^4F_{9/2} \rightarrow {}^6H_{15/2}$), suggesting that the pyridine-2,4,6-tricarboxylato ligand is suitable for the sensitization of the blue luminescence of Dy^{3+} ions. The broad emission band in the region of 340 – 400 nm is due to weak π^*-π or π-n transitions of the organic ligands.

Magnetic properties

The temperature-dependent magnetic susceptibility was measured for the title compound on the a polycrystalline sample in the temperature range of 2 – 300 K in a fixed magnetic field of 5 Koe. It exhibits an interesting magnetic property as shown in Fig. 5 in the form of a $\chi_m T$ *versus* T plot (χ_m being the magnetic susceptibility per two metal ions). It is well known
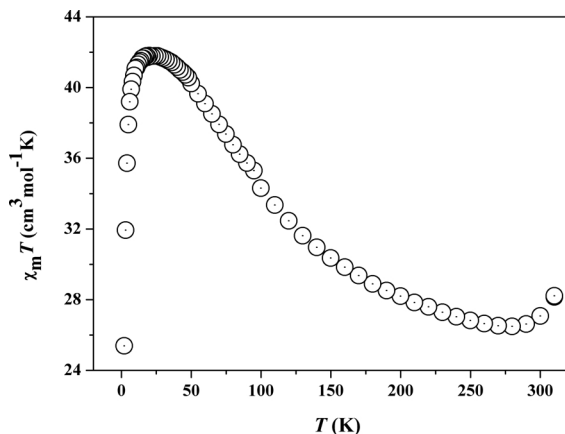

Fig. 5. Temperature dependence of the magnetic susceptibilities of the title compound (χ_m being the magnetic susceptibility per two metal ions).

that, by interelectronic repulsion and spin-orbit coupling, the $4f^n$ configuration of a Ln^{3+} ion is split into $^{2S+1}L_J$ states, and the crystal-field perturbation further leads to the splitting into Stark components. The $\chi_m T$ value at r. t. is *ca.* 28.16 cm^3 K mol^{-1}, close to the expected value of 28.34 cm^3 K mol^{-1} for two isolated Dy^{3+} ions (S = 5/2, L = 5, $^6H_{15/2}$) [23]. This value falls with decreasing temperature, reaching a minimum value of *ca.* 26.49 cm^3 K mol^{-1} at 280 K. A further decrease in temperature causes significant uprising of the $\chi_m T$ value with a maximum of *ca.* 41.80 cm^3 K mol^{-1} at 20 K indicative of ferromagnetic coupling between the Dy^{3+} ions, and subsequently falls sharply to a minimum of *ca.* 25.39 cm^3 K mol^{-1} at 2 K. This profile of the $\chi_m T$ *vs. T* curve suggests the occurrence of two conflicting effects. On the one hand, the decrease in $\chi_m T$ unambiguously originates from the thermal depopulation of the highest Stark levels resulting from the splitting of the 16-fold degenerate $^6H_{15/2}$ ground states by the crystal field, and on the other hand, the antagonist process must be the ferromagnetic interaction between the Dy^{3+} ions. Because of the presence of a large unquenched orbital angular momentum and spin-orbit coupling, it is difficult to estimate the interactions between metal atoms quantitatively, and the origin of this potentially interesting magnetic behavior will be the topic of deeper investigations.

Conclusion

In summary, we have hydrothermally prepared the 3D lanthanide pyridine-2,4,6-tricarboxylato coordination polymer $[Dy_2(H_2O)_5(ptc)_2] \cdot H_2O$. It is a new 3D MOF of an unprecedented topology of $(4 \cdot 6^3 \cdot 8^2)(6^3)$ type. To the best of our knowledge, this compound is the first example of a pyridine-2,4,6-tricarboxylato complex, where the ptc^{3-} anions display two unprecedented coordination modes ($\mu_3\eta^6$ and $\mu_4\eta^6$). The emission spectrum demonstrates the characteristic luminescence of the Dy^{3+} ions upon excitation at 300 nm, suggesting the Dy(III) pyridine-2,4,6-tricarboxylato compound to be a potential candidate for an efficient luminescent material in the visible regions. Further investigations on the magnetic behavior of the title compound are in progress to clarify the roles of crystal field or intermolecular effects.

Experimental Section

Materials

Except pyridine-2,4,6-tricarboxylic acid, which was prepared in high yield by oxidation of 2,4,6-trimethylpyrid-

ine with aqueous alkaline $KMnO_4$ according to a literature method [24], all the other chemicals of reagent grade were commercially available and used without further purification.

Physical methods

Powder X-ray diffraction measurements were carried out with a Bruker D8 Focus X-ray diffractometer to check the phase purity. Single-crystal X-ray diffraction data were collected on a Rigaku Raxis-Rapid X-ray diffractometer. The C, H and N microanalyses were performed with a PE 2400II CHNS elemental analyzer. The FT-IR spectrum was recorded in the range $4000 - 400$ cm^{-1} on a Shimadzu FTIR-8900 spectrometer. The fluorescent spectra were determined on a RF-5301PC fluorophotometer. A thermogravimetric measurement was carried out from r.t. to 800 °C on a pre-weighed sample using a Seiko Exstar 6000 TG/DTA 6300 apparatus with a heating rate of 10 °C min^{-1}. The temperature-dependent magnetic susceptibility was determined with a Quantum Design SQUID magnetomer (Quantum Design Model MPMS-7) in the temperature range $2 - 300$ K with an applied field of 5 kOe, and the susceptibilities were corrected for the diamagnetism of the constituent atoms using Pascal's constants [25].

Synthesis of [Dy₂(H₂O)₅(ptc)₂]·H₂O

15 mL H_2O was added to a mixture of 0.135 g (0.35 mmol) DyCl₃·6H₂O and malonic acid (0.026 g, 0.25 mmol). After the solid material was completely dissolved under continuous stirring, 0.056 g (0.25 mmol) H₃ptc and a solution of 0.056 g (1.00 mmol) KOH in 5 mL H_2O were sucessively added, yielding a colorless precipitate immediately. The mixture was stirred for 30 min, and transferred into a 25 mL Teflon-lined stainless-steel autoclave, which was then heated up to 170 °C, kept at this temperature for 3 d, and then cooled to r.t. After filtration, colorless granule-like crystals of the title compound were obtained (yield: 51 % based on the initial DyCl₃·6H₂O amount). – IR (film): v = 3384m, 3229w, 3081m, 1610w, 1582s, 1551s, 1446s, 1395s, 1353s, 1280m, 1111m, 1026s, 931s, 819m, 792m, 740s, 622w cm^{-1}. – C₁₆H₁₆DyN₂O₁₈ (849.31): calcd. C 22.63, H 1.90, N 3.30; found C 22.40, H 1.82, N 3.41.

X-Ray structure determination

A suitable single crystal was selected under a polarization microscope and fixed with epoxy cement on a fine glass fiber which was then mounted on a Rigaku R-Axis Rapid IP X-ray diffractometer, operating with graphite-monochromatized MoK_α radiation (λ = 0.71073 Å) for cell determination and subsequent data collection. The reflection intensities in the θ range $3.19 - 27.45°$ were collected at 295 K using the ω scan technique. The employed single

Table 2. Crystal structure data for **1**.

Formula	$C_{16}H_{16}DyN_2O_{18}$
M_r	849.31
Crystal size, mm^3	$0.29 \times 0.24 \times 0.17$
Crystal system	monoclinic
Space group	$P2_1/n$
a, Å	18.351(4)
b, Å	6.881(1)
c, Å	18.407(4)
β, deg	110.12(3)
V, Å^3	2182.4(8)
Z	4
D_{calcd}, g cm^{-3}	2.59
$\mu(MoK_\alpha)$, cm^{-1}	6.9
$F(000)$, e	1608
hkl range	$-21 \leq h \leq 21$;
	$-7 \leq k \leq 8$;
	$-21 \leq l \leq 21$
$((\sin\theta)/\lambda)_{max}$, Å^{-1}	0.59
Refl. measured / unique / R_{int}	3841 / 3536 / 0.0826
Param. refined	344
$R1(F)$ / $wR2(F^2)^a$ (all refl.)	0.0374 / 0.0605
GoF $(F^2)^b$	1.100
$\Delta\rho_{fin}$ (max / min), e Å^{-3}	2.22 / -1.16

^{a} $R1 = \Sigma||F_o| - |F_c||/\Sigma|F_o|$, $wR2 = [\Sigma w(F_o^2 - F_c^2)^2/\Sigma w(F_o^2)^2]^{1/2}$, $w = [\sigma^2(F_o^2) + (0.0125P)^2 + 3.6698P]^{-1}$, where $P = (Max(F_o^2,0) + 2F_c^2)/3$; ^{b} GoF = $[\Sigma w(F_o^2 - F_c^2)^2/(n_{obs} - n_{param})]^{1/2}$.

crystal exhibited no detectable decay during the data collection. The data were corrected for Lp and empirical absorption effects. The SHELXS-97 and SHELXL-97 programs were used for structure solution and refinement [26, 27]. The structure was solved by using Direct Methods. Subsequent difference Fourier syntheses enabled all non-hydrogen atoms to be located. After several cycles of refinement, the hydrogen atoms associated with carbon atoms were geometrically generated, and the rest of the hydrogen atoms were located from successive difference Fourier syntheses. Finally, all non-hydrogen atoms were refined with anisotropic displacement parameters by full-matrix least-squares techniques, and hydrogen atoms with isotropic displacement parameters were set to 1.2 times the values for the associated heavier atoms. Detailed information about the crystal data and structure determination is summarized in Table 2.

CCDC 783940 contains the supplementary crystallographic data for this paper. These data can be obtained free of charge from The Cambridge Crystallographic Data Centre *via* www.ccdc.cam.ac.uk/data_request/cif.

[1] H. Tsukube, S. Shinoda, *Chem. Rev.* **2002**, *102*, 2389 – 2403.

[2] R. Nishiyabu, C. Aimé, R. Gondo, T. Noguchi, N. Kimizuka, *Angew. Chem.* **2009**, *121*, 9629 – 9632; *Angew. Chem. Int. Ed.* **2009**, *48*, 9465 – 9468.

[3] P. P. Lima, F. A. A. Paz, R. A. S. Ferreira, V. Z. Bermudez, L. D. Carlos, *Chem. Mater.* **2009**, *21*, 5099 – 5011.

[4] Y. F. Zhou, M. C. Hong, X. T. Wu, *Chem. Commun.* **2006**, 135 – 143.

[5] C. Marchal, Y. Filinchuk, X. Y. Chen, D. Imbert, M. Mazzanti, *Chem. Eur. J.* **2009**, *15*, 5273 – 5288.

[6] Y. Zheng, D. Kustaryono, N. Kerbellec, O. Guillou, Y. Gérault, F. L. Dret, C. Daiguebonne, *Inorg. Chim. Acta* **2009**, *362*, 2123 – 2126.

[7] F. N. Shi, L. Cunha-Silva, R. A. S. Ferreira, L. Mafra, T. Trindade, L. D. Carlos, F. A. A. Paz, J. Rocha, *J. Am. Chem. Soc.* **2008**, *130*, 150 – 167.

[8] X. Li, D. Y. Wei, S. J. Huang, Y. Q. Zheng, *J. Solid State Chem.* **2009**, *182*, 95 – 101.

[9] G. L. Zhuang, X. J. Kong, L. S. Long, R. B. Huang, L. S. Zheng, *CrystEngComm* **2010**, *12*, 2691 – 2694.

[10] P. Wang, J. P. Ma, Y. B. Dong, R. Q. Huang, *J. Am. Chem. Soc.* **2007**, *129*, 10620 – 10621.

[11] N. Kerbellec, D. Kustaryono, V. Haquin, M. Etienne, C. Daiguebonne, O. Guillou, *Inorg. Chem.* **2009**, *48*, 2837 – 2843.

[12] S. K. Ghosh, P. K. Bharadwaj, *Inorg. Chem.* **2004**, *43*, 2293 – 2298.

[13] L. Pan, K. M. Adams, H. E. Hernandez, X. T. Wang, C. Zheng, Y. Hattori, K. Kaneko, *J. Am. Chem. Soc.* **2003**, *125*, 3062 – 3067.

[14] M. C. Das, S. K. Ghosh, E. C. Sañudo, P. K. Bharadwaj, *Dalton Trans.* **2009**, 1644 – 1658.

[15] R. Q. Zou, R. Q. Zhong, M. Du, D. S. Pandey, Q. Xu, *Cryst. Growth Des.* **2008**, *8*, 452 – 459.

[16] C. J. Li, M. X. Peng, J. D. Leng, M. M. Yang, Z. J. Lin, M. L. Tong, *CrystEngComm* **2008**, *10*, 1645 – 1652.

[17] M. V. Yigit, K. Biyikli, B. Moulton, J. C. MacDonald, *Cryst. Growth Des.* **2006**, *6*, 63 – 69.

[18] H. S. Wang, B. Zhao, B. Zhai, W. Shi, P. Cheng, D. Z. Liao, S. P. Yan, *Cryst. Growth Des.* **2007**, *7*, 1851 – 1857.

[19] X. W. Wang, Y. R. Dong, Y. Q. Zheng, J. Z. Chen, *Cryst. Growth Des.* **2007**, *7*, 613 – 615.

[20] Y. R. Dong, X. W. Wang, Y. Q. Zheng, *Acta Crystallogr.* **2007**, *C63*, m19 – m21.

[21] K. Nakamoto, *Infrared and Raman Spectra of Inorganic and Coordination Compounds*, 4th ed., Interscience-Wiley, New York, **1986**.

[22] J. G. G. Bünzli, G. R. Choppin, *Lanthanide Probes in Life, Chemical and Earth Sciences: Theory and Practice*, Elsevier, Amsterdam, **1989**.

[23] R. L. Carlin, *Magnetochemistry*, Springer-Verlag, Berlin, **1986**, pp. 253.

[24] L. Syper, K. Kloc, J. Mochowski, *Tetrahedron* **1980**, *36*, 123 – 129.

[25] G. A. Bain, J. F. Berry, *J. Chem. Educ.* **2008**, *85*, 532 – 536.

[26] G. M. Sheldrick, SHELXS-97, Program for the Solution of Crystal Structures, University of Göttingen, Göttingen (Germany) **1997**. See also: G. M. Sheldrick, *Acta Crystallogr.* **1990**, *A46*, 467 – 473.

[27] G. M. Sheldrick, SHELXL-97, Program for the Refinement of Crystal Structures, University of Göttingen, Göttingen (Germany) **1997**. See also: G. M. Sheldrick, *Acta Crystallogr.* **2008**, *A64*, 112 – 122.